Frequency Response of the CSIRO Liquid Water Probe

S. G. BRADLEY AND W. D. KING

Division of Cloud Physics, CSIRO, Sydney, Australia

(Manuscript received 24 July 1978, in final form 22 November 1978)

ABSTRACT

A recent treatment of the dynamic behavior of anemometer hot wires is simplified and used to show that the response of the CSIRO liquid-water hot wire can be described by a second-order differential equation. This is confirmed by experiment, and it is shown that the inherent time scale is fully calculable in terms of the thermal properties of the wire and its support and the amplifier constants. For most clouds a response time of 0.005 s can be readily achieved.

1. Introduction

Twomey (1976) has shown that the small regions of cloud with higher-than-average liquid water content can account for many of the larger drops formed through the coalescence process. For example, if 1% of the cloud experiences liquid water values of 3 g m^{-3} for a few minutes, then these regions can produce concentrations of larger drops which are 10^9 times higher than elsewhere in the cloud. It is therefore important to measure fluctuations in liquid water as well as the mean value, and with a frequency response of better than 10 Hz. While the fine wires of the JW and NOAA liquid-water devices should readily satisfy this criterion, the construction of the CSIRO hot-wire element (King *et al.*, 1978), with its large thermal mass, is such that a response time of many seconds would be expected. It is the purpose of this paper to demonstrate that the response time of the element can be as short as 5 ms to outline the parameters determining this response and to describe a test procedure which enables this response to be obtained with minimum effort.

2. The hot wire and its control circuit

Construction of the CSIRO hot-wire element has been described by King *et al.* (1978). Its main features are a central sensing element 3.8 cm long consisting of 0.102 mm diameter copper wire close wound on a nickel-silver tube of 1.6 mm diameter. At either end of this sensing coil there is a similar slave coil 1.9 cm long whose function is to reduce axial heat losses. The wire is maintained at a constant temperature of about 100°C via a control circuit, and under these conditions the total power transferred from the wire to its environment is

$$P=\mathrm{Nu}\pi lk(T_w-T_a)+lduw[L+c(T_w-T_a)], \quad (1)$$

where Nu is the Nusselt number for air flow past the cylinder at velocity u, l and d the length and diameter of the sensing element, k is the thermal conductivity of air, w the liquid-water content, L and c the latent and specific heats of water, and T_w and T_a the temperature of the wire and air. At a speed of 60 m s^{-1} and with $T_w=100$°C and $T_a=0$°C, the two terms on the right-hand side of (1) are equal when the liquid-water content is $\sim$1.5 g m^{-3}.

The constant-temperature control circuit is shown in Figs. 1 and 2. The temperature of the wire is sensed through its resistance in the bridge. Any cooling of the wire decreases its resistance, leading to an increased voltage at the top of the bridge via the feedback amplifier. The wire is thus heated until the balance point is again achieved. The offset capability shown in Fig. 1 is an important feature of the circuit, as will be shown later, but the voltage V_t is used for test and setup purposes only.

This circuit is similar to those used to control hotwire anemometers, and in the following we will use a treatment developed by Freymuth (1977a) for describing the dynamic behavior of such anemometers.

The equations governing the behavior of the wire are as follows:

1) HEAT BALANCE OF THE WIRE

$$\frac{V_s^2R}{(R+R_1)^2}-P=h\frac{dT_w}{dt}=-\frac{h}{\alpha}\frac{dR}{dt}, \quad (2)$$

where V_s is the bridge voltage, R the hot-wire resistance, R_1 a bridge resistor as shown in Fig. 1, P the heat loss from the wire according to (1), h the heat capacity of the wire and support, and α the temperature coefficient of resistance of the wire. In equilibrium, $P=V_s^2R/(R+R_1)^2$.

0021-8952/79/030361-06$05.50
© 1979 American Meteorological Society

Unauthenticated | Downloaded 03/27/23 11:23 AM UTC

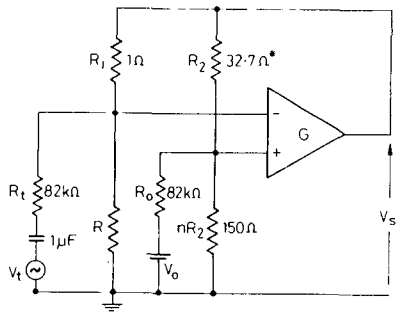

FIG. 1. The hot-wire bridge and feedback control loop. The resistance with the asterisk has been adjusted for a wire temperature of 100°C.

2) BRIDGE VOLTAGE

$$V_{in}=\frac{V_s(nR_1-R)}{(n+1)(R_1+R)}+\frac{n}{n+1}\frac{R_2}{R_0}V_0-\frac{n}{n+1}\frac{R_1}{R_t}V_t. \tag{3}$$

3) AMPLIFIER RESPONSE

$$\tau_1\tau_2\frac{d^2V_s}{dt^2}+(\tau_1+\tau_2)\frac{dV_s}{dt}+V_s=GV_{in}. \tag{4}$$

Here we have assumed the amplifier has a zero-frequency gain of G, with two poles at frequencies of $(2\pi\tau_1)^{-1}$ and $(2\pi\tau_2)^{-1}$, where $\tau_2<\tau_1$. The input offset voltage of the amplifier has been incorporated in the V_0 term in (3).

The above three equations can be combined and linearized for small signal deviations from the equilibrium values to yield a single dynamic equation on which most of Freymuth's (1977a) analysis is based, i.e.,

$$\frac{\tau_w\tau_1\tau_2}{G}\frac{d^3v}{dt^3}+\frac{\tau_w(\tau_1+\tau_2)}{G}\frac{d^2v}{dt^2}+\tau_w\frac{nR_2}{(n+1)R_0}\frac{V_0}{V_s}\frac{dv}{dt}+v$$
$$=\frac{V_s}{2}\frac{p}{P}+\tau_w\frac{nR_1}{(n+1)R_t}\frac{dV_t}{dt}, \tag{5}$$

where v and p are small departures from the equilibrium values of V_s and P, respectively, and τ_w a small-signal time constant associated with the wire and defined by

$$\tau_w=\frac{(n+1)^2}{2}\frac{R_1h}{\alpha P}. \tag{6}$$

An important simplification of (5) can be made when the maximum frequency of the forcing term p is much less than τ_2^{-1}. Then the contribution of the first term (5) is much less than that of the second. (For the CSIRO amplifier we have $\tau_2\ll10^{-6}$ s, so that even for cloud elements of 10 cm scale sampled at an airspeed of 60 m s^{-1}, the above condition is easily met. It should be noted, however, that this implies the use of a wide-band amplifier, and the 2N5830 driver in Fig. 2 ensures $\tau_2\ll10^{-6}$ s when 5 A is being drawn from the TIP 141 at high liquid-water values.) With this simplification, and noting $\tau_2\ll\tau_1$, we can reduce (5) to a second-order differential equation which can be expressed in the following standard form for a damped harmonic oscillator

$$\frac{d^2v}{dt^2}+2\zeta\omega_n\frac{dv}{dt}+\omega_n^2v=\frac{\omega_n^2}{2}\frac{p}{P}V_s+\frac{GnR_1}{\tau_1(n+1)R_t}\frac{dV_t}{dt}, \tag{7}$$

where

$$\omega_n=(G/\tau_w\tau_1)^{\frac{1}{2}}, \tag{8}$$

$$\zeta=\frac{nR_2}{(n+1)R_0}\left(\frac{G\tau_w}{\tau_1}\right)^{\frac{1}{2}}\frac{V_0}{2V_s}. \tag{9}$$

Here ω_n is the frequency of natural oscillations of the system (i.e., ω_n^{-1} is the natural time scale) and ζ the damping factor.

Since a system described by (7) will oscillate at frequency ω_n for zero or negative damping factor, (9) shows that a net positive offset voltage is required for stable operation of the circuit. The three base-emitter voltage drops contribute a small, negative offset voltage and the operational amplifier will also have an output offset. These inherent circuit offset voltages are readily trimmed out, and the circuit can be critically damped ($\zeta=1$) for values of V_0 in the range 1–10 V.

The validity of the small-signal approximation in the derivation of (7) is examined in the Appendix. It is found that (7) adequately describes the wire response except for very large, fast changes of cooling. The small-signal analysis, therefore, will be the basis for further description of the behavior of the wire.

3. Determination of τ_w

As shown in (6), τ_w is not constant but depends inversely on the equilibrium heat loss. Since τ_w is of fundamental importance in determining wire frequency

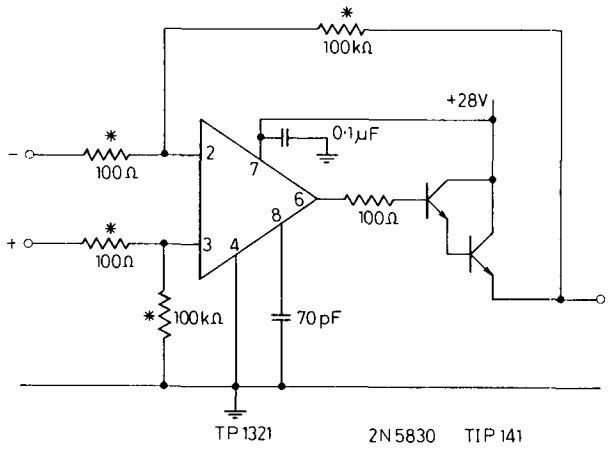

FIG. 2. Details of the wide bandwidth×1000 amplifier. Values with asterisks represent matched resistors.

Unauthenticated | Downloaded 03/27/23 11:23 AM UTC

response, we will now show how τ_w may be both calculated and measured. The following paragraphs refer to minimum heat loss and hence maximum τ_w. At aircraft speeds, τ_w would be at least an order of magnitude smaller.

a. Direct calculation of τ_w

From the mass of the hot wire and support, and assuming specific heats of 400 and 300 J kg^{-1} °C^{-1} for copper and nickel silver, respectively, we obtain a total thermal capacity h of 0.10 J °C^{-1}. In still air and under equilibrium conditions, V_s was measured as 2.45V. From (2) and (6) we therefore find $\tau_w = 350 \pm 100$ s. The large estimated error is due to the inaccuracy of specific heats.

b. Direct measurement of τ_w

When there is zero voltage across the wire (2) and (6) may be combined to give

$$\tau_w = \frac{(n+1)^2}{2} \frac{R_1}{dR/dt}. \tag{10}$$

Fig. 3 shows the decay of R with time as the wire cools after being heated above the normal operating temperature. When both the sensing element and the slave coils are heated, the slope at $R = nR_1$ yields $\tau_w = 300 \pm 30$ s, in good agreement with the value obtained in 3.1. However, when only the sensing coil is heated we obtain $\tau_w = 150 \pm 30$ s, the reduction in τ_w being due to axial heat loss through the support tube.

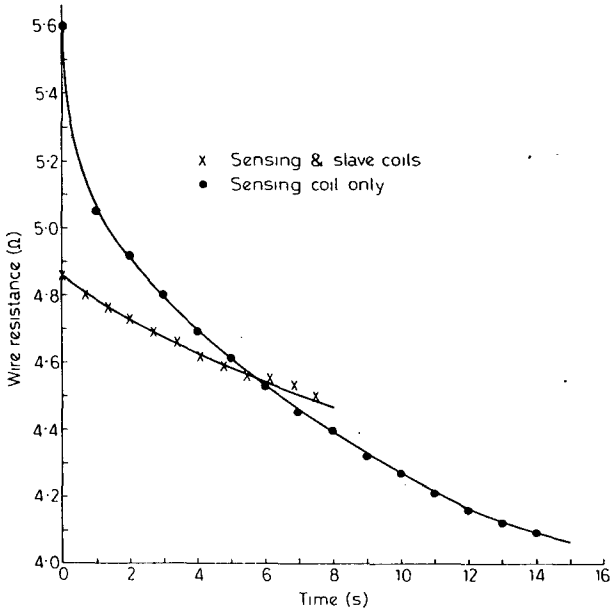

FIG. 3. The rate of cooling of the wire and support in still air.

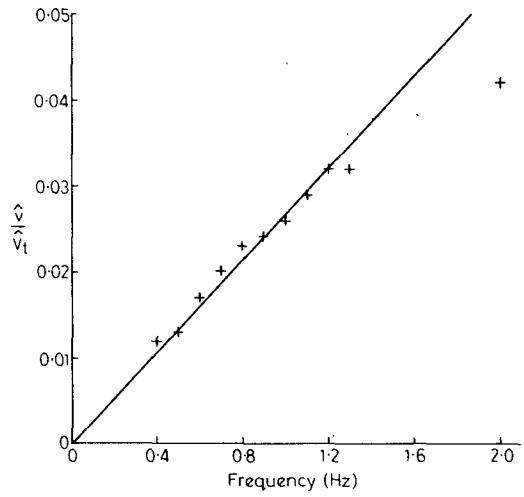

FIG. 4. Variation of gain with frequency for a sinusoidal test signal.

c. The sine-wave test

Freymuth (1977a) used a sinusoidal test signal input $V_t = \hat{V}_t \sin 2\pi f$ to determine the wire time constant. For low frequencies (5) becomes

$$v = \tau_w \frac{nR_1}{(n+1)R_t} \frac{dV_t}{dt}. \tag{11}$$

For a sinusoidal input, rearrangement yields

$$\tau_w = \frac{n+1}{n} \frac{R_t}{R_1} \frac{1}{2\pi \hat{V}_t} \frac{d\hat{v}}{df}, \tag{12}$$

where $\hat{v}$ is the output voltage amplitude. In Fig. 4 the measured output amplitude is shown as a function of frequency. Since the slave coils were not connected the calculated $\tau_w = 150 \pm 20$ s is in excellent agreement with the corresponding measurement in Section 3b.

We find good agreement between the above three methods for finding τ_w. It is therefore possible to calculate τ_w from a knowledge of wire geometry and thermal properties, and this, together with information on the amplifier gain-bandwidth product, enables the time scale for the wire response to be fully calculable.

4. Response to a step test input

The technique used by Freymuth (1977a) to optimize a third-order circuit can be adapted to critically damp the present circuit. A step input V_t is introduced across the bridge, resulting in an output voltage

$$v = \frac{v_0}{2a}\{\exp[-\omega_n(\zeta - a)t] - \exp[-\omega_n(\zeta + a)t]\}, \quad [\zeta > 1], \tag{13}$$

$$v = v_0 \omega_n t \exp(-\omega_n t), \quad [\zeta = 1], \tag{14}$$

$$v = \frac{v_0}{a} \exp(-\zeta \omega_n t) \sin(a\omega_n t), \quad [\zeta < 1], \tag{15}$$

Unauthenticated | Downloaded 03/27/23 11:23 AM UTC

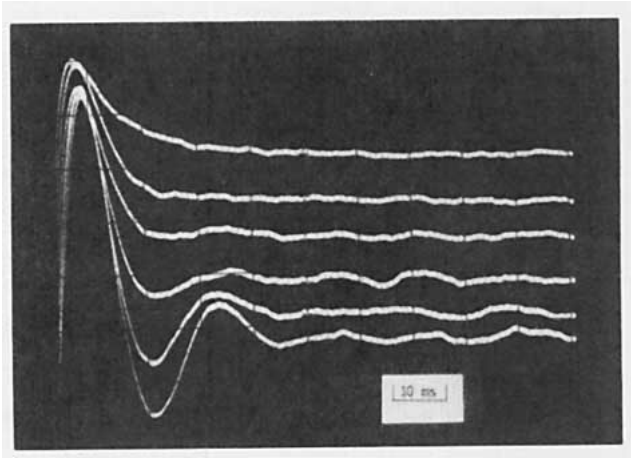

FIG. 5. Oscilloscope traces showing the output waveform variation with adjustment of offset voltage V_0. From top to bottom, V_0=0.4, 0.0, −0.1, −0.2, −0.4, −0.5 V. Time scale 10 ms per division.

where

$$a=|(\zeta^2-1)^{\frac{1}{2}}|, \tag{16}$$

$$v_0=-\omega_n\tau_w\frac{nR_1}{(n+1)R_t}\hat{V}_t \tag{17}$$

and $\hat{V}_t$ is the amplitude of the input step. The circuit is critically damped when undershoot oscillations just disappear and $\zeta=1$. Fig. 5 shows the output waveform variation with adjustment of offset voltage V_0. If V_0 is such as to cancel the input offset voltage inherent in the circuit, then $\zeta=0$ and (15) predicts undamped oscillations. The period of these oscillations was found to be ~0.02 s, giving $\omega_n=314$ s^{-1}, in agreement with earlier computations. Using (6) to eliminate τ_w from (9) and (2) to eliminate P for steady-state conditions, we obtain

$$V_s^2=\frac{(n+1)R_1R_2}{2\zeta R_0}\left(\frac{nhG}{2\alpha\tau_1}\right)^{\frac{1}{2}}V_0. \tag{18}$$

When the steady-state output voltage was measured, together with input offset V_0 for critical damping at various cooling rates, the curve shown in Fig. 6 was obtained. The expected square-law is followed and enables the offset voltage for critical damping to be predicted for any circuit operating point.

5. Response to a step change in liquid water

For small test signals the outputs following either a step increase or a step decrease are similar. However, the output following a step decrease in liquid water will change more slowly than for a step increase, because of the time taken to evaporate droplets. Provided the evaporation time is longer than ω_n^{-1}, the equilibrium form of (2) describes the output voltage change.

Consider a droplet that impinges on the wire, beads up hemispherically, is not ventilated, and is maintained at the wire temperature. Then according to King *et al.* (1978), the radius of the drop as a function of time is

$$a(t)=a_0[1-t/\tau(a_0)]^{\frac{1}{2}}, \tag{19}$$

where a_0 is the initial droplet radius and $\tau(a_0)$ is the evaporation time, given by

$$\tau(a_0)=(a_0/\gamma)^2, \tag{20}$$

$$\gamma^2=\frac{D[\rho_s(T_w)-\rho_s(T_a)]}{\rho_w}. \tag{21}$$

Here ρ_w is the density of water, D the diffusivity of water vapor in air and $\rho_s(T)$ the saturated vapor density of water at temperature T.

Now the power delivered to a droplet of mass m will be

$$P(a_0,t)=-L\frac{dm}{dt}=4\pi L\gamma^2\rho_w a_0[1-t/\tau(a_0)]^{\frac{1}{2}}. \tag{22}$$

Consider now a distribution of droplet size described by $n(a_0)da_0$, the number of droplets having radii between a_0 and a_0+da_0. If this distribution is placed on the wire at $t=0$, then the total power delivered is

$$P(t)=4\pi L\gamma^2\rho_w\int_{a_m}^{\infty}a_0[1-t/\tau(a_0)]^{\frac{1}{2}}n(a_0)da_0, \tag{23}$$

where the lower limit of integration a_m is the initial size of the smallest droplet remaining at time t. From (20),

$$a_m=\gamma t^{\frac{1}{2}}. \tag{24}$$

In an experiment to confirm the formula (23) a short "puff" of liquid water was sprayed on to the wire in a wind tunnel operating at 40 m s^{-1}. A typical example of bridge output V_s is shown in Fig. 7. The droplet

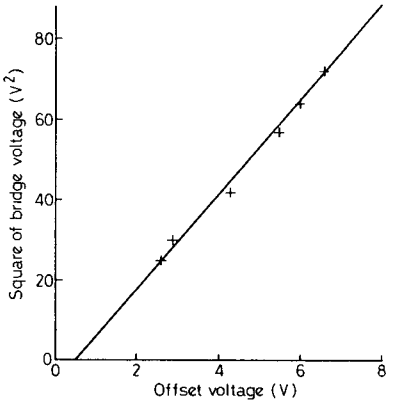

FIG. 6. The offset voltage V_0 for critical damping at various heat loads, as a function of V_s.

Unauthenticated | Downloaded 03/27/23 11:23 AM UTC

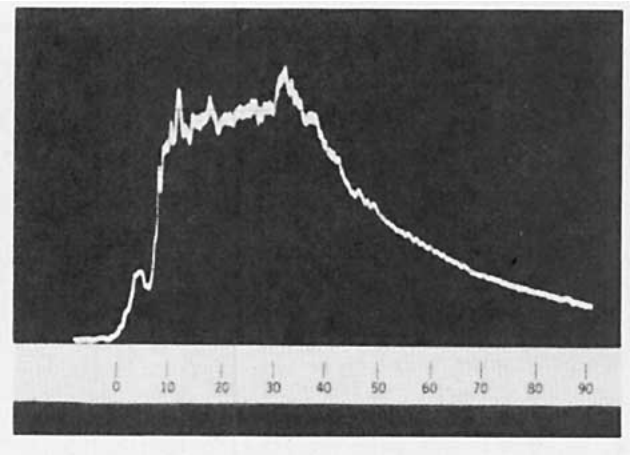

FIG. 7. An example of hot-wire response to a short burst of liquid water. The time scale is 10 ms per division.

spectrum was measured using soot slides and was found to be approximately Gaussian with mean diameter 32 μm and standard deviation 13 μm. The theoretical V_s curve for this distribution is shown in Fig. 8, together with the observed decay. It is clear that the form of the decay is closely described by (23) but that the real decay was somewhat faster than the calculated one. The discrepancy is probably due to neglecting ventilation in the derivation of (23).

It is apparent that the overall hot-wire response will depend on the evaporation time constant τ and ω_n^{-1}, the larger parameter dominating. An examination of Fig. 8 together with (20) shows that for most clouds (for which the mean droplet diameter will be <16 μm), both τ and ω_n^{-1} will be of the order of 0.005 s, and we could therefore expect a system response of this order. For clouds whose mean droplet diameter exceeds ~ 16 μm, the evaporation time will dominate, but the total response time is still unlikely to exceed ~ 0.030 s.

It should also be noted that the effect of a single, large drop impinging on the wire will not be interpreted as a large step change in liquid water. Its effect will be to raise the power output a very small amount, but for the extended residence time predicted by (20). The fractional change in power is approximately equal to

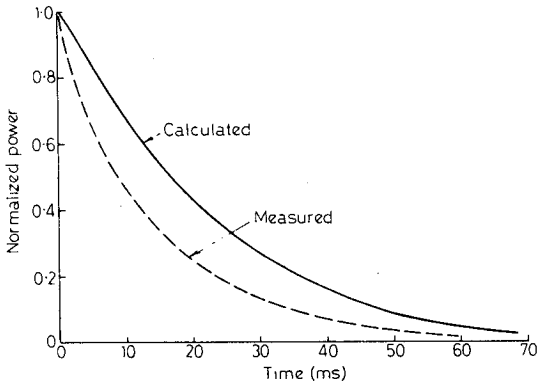

FIG. 8. The decay of V_s following a short burst of liquid water.

the ratio of the volume of the drop to that of the total water accumulated during the residence time.

6. Conclusions

The following points emerge from the work described in this paper:

1) The small-signal approximation provides an adequate basis for describing the behavior of the hot-wire and feedback loop.

2) Provided the amplifier has a high gain-bandwidth product at currents up to $5A$, the system is described by a second-order differential equation.

3) The basic time scale for the system response is fully calculable in terms of wire geometry and thermal properties and amplifier characteristics.

4) A net positive offset voltage is mandatory for loop stability.

Since amplifier offsets vary from chip to chip, the following scheme is recommended for optimizing the control loop. Using a step test input, adjust V_0 for critical damping and note V_s. Repeat this procedure with a range of heat loads achieved, say, by applying a damp cloth to the wire. A plot of $V_0(\zeta=1)$ versus V_s^2 is obtained. Extrapolate this curve to determine the value of V_0 required for critical damping at the highest value of V_s expected [use Eqs. (1) and (2) to relate V_s, liquid water content, and air speed]. This is a conservative design criterion, since the system will then be overdamped at all values of liquid water content.

If the above procedures are followed and the wire operating temperature is near 100°C, a response time of 5 ms will be obtained. Even if G/τ_1 is two orders of magnitude smaller than used here, a response time of 50 ms will be achieved.

APPENDIX

Large-Amplitude Changes in Liquid Water

The linearized Eq. (7) was derived assuming small changes in power, output voltage and wire resistance. While a large change in power will result in a large change in output voltage, the wire resistance is maintained very close to the balance value because of the large loop gain of the system. We will now show that the assumption of small changes in wire resistance is valid, and solve Eqs. (2), (3) and (4) under these conditions. Instead of solving directly in terms of V_s, we will solve in terms of scaled liquid water w_s, defined by

$$w_s = \frac{nV_s^2}{(n+1)^2 R_1 A} - \frac{B}{A}, \tag{A1}$$

where A and B are coefficients in (1) when rewritten as

$$P = Aw + B. \tag{A2}$$

Unauthenticated | Downloaded 03/27/23 11:23 AM UTC

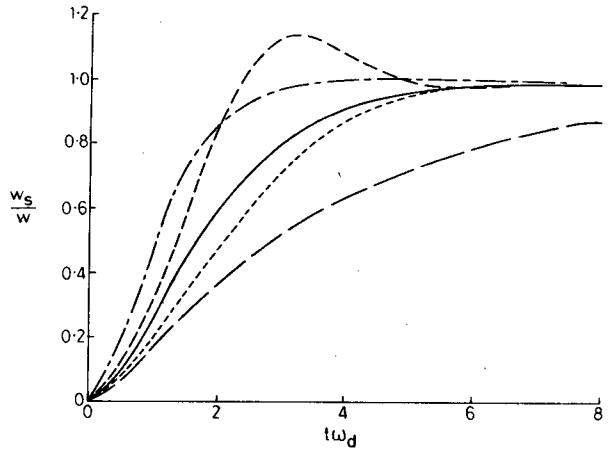

FIG. 9. Response of the hot wire to finite step changes in liquid water: (——)$\zeta_d=1$, w small; (— —)$\zeta_d=1$, $w=B/A$; (— — —)$\zeta_d=1$, negative step from $w=B/A$ to $w=0$; (– –)$\zeta_d=2$, w small; (- - - -)$\zeta_d=2$, $w=B/A$.

The scaled liquid water is the liquid water value inferred from measurements of V_s, assuming "ideal" conditions of a balanced bridge.

Following Freymuth (1977b), we first define the quantity δ by

$$\delta=\frac{nR_1-R}{R_1+R} \tag{A3}$$

and obtain

$$\frac{dR}{dt}=-\frac{(n+1)}{(1+\delta)^2}R_1\frac{d\delta}{dt}. \tag{A4}$$

Substituting for dR/dt in (2) and using (A2) yields

$$w=w_s(1+\delta)(1-\delta/n)+\frac{B}{A}\delta\left(1+\frac{1-\delta}{n}\right)+\frac{(n+1)hR_1}{\alpha A(1+\delta)^2}\frac{d\delta}{dt}. \tag{A5}$$

We now wish to express δ in terms of w_s. Eqs. (3) and (4) can be rewritten

$$\delta=\frac{n+1}{G}\left(1-G\frac{nR_2}{(n+1)R_0}\frac{V_0}{V_s}+\frac{\tau_1}{V_s}\frac{dV_s}{dt}\right). \tag{A6}$$

By substituting w_s for V_s in (A6) from (A1) and inserting δ into (A5) after some rearrangement, we obtain

$$w=w_s(1+\delta)(1-\delta/n)+\frac{B}{A}\delta\left(1+\frac{1-\delta}{n}\right)+\frac{\beta^3}{(1+\delta)^2}\times\frac{2\zeta_d}{\omega_d}\frac{dw_s}{dt}+\frac{\beta^2}{(1+\delta)^2}\frac{1}{\omega_d^2}\frac{d^2w_s}{dt^2}-\frac{A\beta^4}{B\omega_d^2(1+\delta)^2}\left(\frac{dw_s}{dt}\right)^2, \tag{A7}$$

where

$$\beta=(1+Aw_s/B)^{-\frac{1}{2}}, \tag{A8}$$

$$\zeta_d=\frac{nR_2}{(n+1)R_0}\left(\frac{G\tau_d}{\tau_1}\right)^{\frac{1}{2}}\frac{V_0}{2V_d}, \tag{A9}$$

$$\omega_d=(G/\tau_1\tau_d)^{\frac{1}{2}}, \tag{A10}$$

$$V_d^2=\frac{(n+1)^2}{n}R_1B, \tag{A11}$$

$$\tau_d=\frac{(n+1)^2}{2}\frac{R_1h}{\alpha B}. \tag{A12}$$

The quantities ζ_d, ω_d, V_d and τ_d are, respectively, the damping factor, natural frequency, output voltage and wire time constant in a steady, dry airflow.

Equation (A7) is exact, but is simplified greatly if δ is small. Substituting known values for the constants in (A6) and assuming that V_s does not change by more than a factor of 2 in time ω_d^{-1}, we find $\delta<6\times10^{-3}$. Consequently, to within about 1%, (A7) may be written

$$w=w_s+\beta^3\frac{2\zeta_d}{\omega_d}\frac{dw_s}{dt}+\frac{\beta^2}{\omega_d^2}\frac{d^2w_s}{dt^2}-\frac{A\beta^4}{B\omega_d^2}\left(\frac{dw_s}{dt}\right)^2. \tag{A13}$$

For small changes in liquid water content, w_s therefore obeys a second-order differential equation identical in form to (7). For large, fast changes the scaled liquid water w_s deviates from actual liquid water w in a more complicated fashion. Eq. (A13) has been solved for a step increase in w and for ζ_d values of 1 and 2. Unity ζ_d corresponds to critical damping under conditions of zero liquid water, whereas a value of 2 corresponds to critical damping at $w=B/A$ or approximately 1.5 g m^{-3}. To explore further the nonlinear behavior, (A10) was solved for a step *decrease* in w. The conclusion from the solutions shown in Fig. 9 is that the nonlinear terms produce marked departures from the linearized solution for large fast changes; the response being less damped. Overshoot for the less conservative damping is about 13% but undershoot is negligible. Although it is extremely unlikely that a 1.5 g m^{-3} step in liquid water will be met in practice, we prefer to adopt the more conservative damping ($\zeta_d=2$) corresponding to critical damping at a high level of liquid water content. The frequency response is then never peaked and the 3 dB cutoff frequency will lie between about 250 and 350 Hz.

REFERENCES

Freymuth, P., 1977a: Frequency response and electronic testing for constant-temperature hot-wire anemometers. *J. Phys. E, Sci. Instrum.*, **10**, 705–10.

——, 1977b: Further investigation of the nonlinear theory for constant-temperature hot-wire anemometers. *J. Phys. E, Sci. Instrum.*, **10**, 710–13.

King, W. D., D. A. Parkin and R. J. Handsworth, 1978: A hot-wire liquid water device having fully calculable response characteristics. *J. Appl. Meteor.*, **17**, 1809–1813.

Twomey, S., 1976: The effects of fluctuations in liquid water content on the evolution of large drops by coalescence. *J. Atmos. Sci.*, **33**, 720–723.

Unauthenticated | Downloaded 03/27/23 11:23 AM UTC